Nuclear transporters in a multinucleated organism: functional and localization analyses in *Aspergillus nidulans*

Ane Markina-Iñarrairaegui[a], Oier Etxebeste[a,*], Erika Herrero-García[a], Lidia Araújo-Bazán[a], Javier Fernández-Martínez[a,†], Jairo A. Flores[a], Stephen A. Osmani[b], and Eduardo A. Espeso[a]
[a]Department of Cellular and Molecular Medicine, Centro de Investigaciones Biológicas, National Research Council, 28040 Madrid, Spain; [b]Department of Molecular Genetics, Ohio State University, Columbus, OH 43210

ABSTRACT **Nuclear transporters mediate bidirectional macromolecule traffic through the nuclear pore complex (NPC), thus participating in vital processes of eukaryotic cells. A systematic functional analysis in *Aspergillus nidulans* permitted the identification of 4 essential nuclear transport pathways of a hypothetical number of 14. The absence of phenotypes for most deletants indicates redundant roles for these nuclear receptors. Subcellular distribution studies of these carriers show three main distributions: nuclear, nucleocytoplasmic, and in association with the nuclear envelope. These locations are not specific to predicted roles as exportins or importins but indicate that bidirectional transport may occur coordinately in all nuclei of a syncytium. Coinciding with mitotic NPC rearrangements, transporters dynamically modified their localizations, suggesting supplementary roles to nucleocytoplasmic transport specifically during mitosis. Loss of transportin-SR and Mex/TAP from the nuclear envelope indicates absence of RNA transport during the partially open mitosis of *Aspergillus*, whereas nucleolar accumulation of Kap121 and Kap123 homologues suggests a role in nucleolar disassembly. This work provides new insight into the roles of nuclear transporters and opens an avenue for future studies of the molecular mechanisms of transport among nuclei within a common cytoplasm, using *A. nidulans* as a model organism.**

Monitoring Editor
Karsten Weis
University of California, Berkeley

Received: Mar 30, 2011
Revised: Jul 27, 2011
Accepted: Aug 19, 2011

INTRODUCTION

The nucleus is the characteristic organelle of eukaryotic cells. A double membrane, the nuclear envelope (NE), surrounds the nucleus and separates the genetic material from the cytoplasm. The nucleoplasm and cytoplasm communicate through multiprotein nuclear pores inserted at the NE. Nuclear pore complexes (NPCs; Ryan and Wente, 2000) are 60- to 125-MDa structures in vertebrates (Cronshaw *et al.*, 2002) and 22–44 MDa in *Saccharomyces cerevisiae* (Rout *et al.*, 2000).

The NPC allows free diffusion of molecules smaller than 30 kDa (Gorlich and Kutay, 1999). However, macromolecule transport is an energy-requiring process that demands the participation of specific nuclear carriers. The majority of these transporters, also called receptors, belong to the karyopherin-β superfamily and are commonly called karyopherins (KAPs). Fifteen importin-β1–like proteins have been identified in yeast and 22 in mammals (Strom and Weis, 2001; Mosammaparast and Pemberton, 2004). Karyopherins mediate the bidirectional transport of most nuclear proteins between the nucleus and the cytoplasm and the export and import of specific types of RNAs. The repetition of a HEAT repeat within the amino acid chain of KAPs allows the formation of a helical structure that permits the simultaneous interaction with cargoes and constituents of the NPC (Chook and Blobel, 2001; Suntharalingam and Wente, 2003; Madrid and Weis, 2006). Therefore these protein carriers may be considered as transient components of the NPC.

This article was published online ahead of print in MBoC in Press (http://www.molbiolcell.org/cgi/doi/10.1091/mbc.E11-03-0262) on August 31, 2011.

Present addresses: *Department of Applied Chemistry, Faculty of Chemistry, University of the Basque Country, 20018, San Sebastian, Spain; †Laboratory of Cellular and Structural Biology, Rockefeller University, New York, NY 10065.

Address correspondence to: Eduardo A. Espeso (eespeso@cib.csic.es).

Abbreviations used: An-Fib, *Aspergillus nidulans* fibrillarin; DAPI, 4′,6-diamidino-2-phenylindole; DsRed, tetrameric *Discosoma* species red fluorescent protein; GFP, green fluorescent protein; KAP, karyopherin; mCh, monomeric cherry red fluorescent protein; NE, nuclear envelope; NES, nuclear export signal; NLS, nuclear localization signal; NPC, nuclear pore complex; NUP, nucleoporin; SPB, spindle pole body.

Structural and functional characterization of importin-β1 allowed the generation of a model that has been extrapolated to the rest of the KAPs (Chook and Blobel, 2001). Nuclear transporters are divided into importins—those mediating the transport from the cytoplasm to the nucleus—and exportins, which play the reverse role (Strom and Weis, 2001). Molecular cargoes to be imported into the nucleus may contain, at least, a nuclear localization signal (NLS). Of these, the best characterized are the so-called classic NLS sequences recognized by importin-α and are essentially composed of basic amino acids, Lys and Arg (Makkerh *et al.*, 1996). Depending on the number of basic residue clusters, classic NLSs are classified as monopartite (Kalderon *et al.*, 1984) or bipartite (Robbins *et al.*, 1991). However, importin-α may recognize alternative NLSs (Kosugi *et al.*, 2009). Cytoplasmic proteins that demand a timely regulation of nuclear exit contain nuclear export signals (NESs; Mattaj and Englmeier, 1998; Macara, 2001; Pemberton and Paschal, 2005). Classic NESs are recognized by exportin 1/Xpo1/CRM1p family transporters and are rich in Leu residues (Fornerod *et al.*, 1997; Ossareh-Nazari *et al.*, 1997; Stade *et al.*, 1997; Neville and Rosbash, 1999). Classic NLSs or NESs are predictable by direct comparison with well-established consensus sequences, and appropriate online search engines have been developed (la Cour *et al.*, 2004; Nguyen Ba *et al.*, 2009). However, the nuclear export and import signals recognized by the other KAPs are less predictive, and empirical approaches are usually required. Two additional transport pathways, largely divergent from KAPs, have also been defined. Certain mRNAs are exported by the MEX/NXT heterodimer (Macara, 2001). The import of the small Ras-type GTPase Ran (Ras nuclear), a key element for nuclear transport (see later discussion), is mediated by the nuclear transport factor Ntf2p/NTF2, which is closely related to the Mex and Nxt receptors (Macara, 2001).

The energy required for nuclear transport is supplied by the asymmetric distribution of the Ran GTPase. The cytoplasmic concentration of GTP-bound Ran (Ran-GTP) is low because it rapidly converts into Ran-GDP. In contrast, the nuclear Ran-GTP concentration is elevated. This nucleocytoplasmic gradient is generated by Ran cofactors (Mattaj and Englmeier, 1998; Gorlich and Kutay, 1999; Macara, 2001). Ran guanine nucleotide exchange factor (RanGEF) is a chromatin-associated nuclear protein (Ohtsubo *et al.*, 1989) that catalyzes Ran GDP-to-GTP exchange. Ran-GTPase activating protein (RanGAP) is a cytoplasmic protein that activates Ran GTPase activity (Bischoff *et al.*, 1995). Importins bind NLS-containing cargoes in the cytoplasm under low Ran-GTP conditions. In the nucleus the cargo/importin heterocomplex is disassembled by the interaction with Ran-GTP, with the subsequent release of the cargo in the nucleoplasm (Petosa *et al.*, 2004). Exportins bind NES-containing proteins in the nucleus due to the presence of a higher Ran-GTP concentration. Once in the cytoplasm, the GTP-to-GDP hydrolysis induced by RanGAP causes the release of the cargo (Mattaj and Englmeier, 1998; Gorlich and Kutay, 1999; Macara, 2001; Weis, 2002). Ran-GDP is then imported in the nucleus by Ntf2p/NTF2 action, completing the transport cycle.

The NE remains intact, but NPCs undergo a partial disassembly during mitosis in *Aspergillus nidulans* (De Souza and Osmani, 2007; Osmani *et al.*, 2006a). Nucleoporins (NUPs) are the elements constituting the basic structure of the NPC and are organized within the pore into three main substructures (Ryan and Wente, 2000): 1) Concentric rings formed by a "core" of structural NUPs that anchor the NPC to the membrane. 2) Radial symmetric modules allowing expansion of the NPC structure toward both the cytoplasm and the nucleoplasm. 3) NUPs organized into flexible filaments that generate the specific environment inside the pore for the translocation of transporter/cargo heterocomplexes in or out of the nucleus. The exact mode of transport through the NPC remains unknown, and three models have been proposed: Brownian movement (Rout *et al.*, 2000), hydrophobic exclusion (Ribbeck and Gorlich, 2002), and "oily spaghetti" (Macara, 2001). "Core" or structural NUPs remain at the NE during mitosis in *A. nidulans*, but the more peripheral NUPs generally disperse, allowing free diffusion of macromolecules between nucleus and cytoplasm at this phase (De Souza and Osmani, 2007; Osmani *et al.*, 2006a). Besides these changes in NPC composition, the nucleolus segregates in a unique manner during mitosis in *A. nidulans*. The nucleolus is first compartmentalized away from DNA during DNA segregation at anaphase. The nucleolar proteins are then disassembled into the cytoplasm and are translocated to daughter nuclei for subsequent regeneration of nucleoli (Ukil *et al.*, 2009).

In this work we present the first functional and localization analysis of the nuclear transport machinery in a multinucleated cell. The *A. nidulans* "nuclear-transportome," defined as the collection of nuclear transporters, has been studied by generating strains carrying single null alleles for each carrier. This reverse genetic study has allowed the identification of essential and nonessential nuclear transport pathways for a coenocytic cell. Cellular distributions were investigated by the generation of endogenous fluorescent fusions. Nuclear transporters are associated with every nucleus of the syncytium during interphase, but distribution changes during mitosis and specific locations for several carriers are observed. Overall the data indicate how nuclear transport might occur and suggest possible roles for some of these transporters outside of nuclear transport in a model filamentous fungal cell.

RESULTS

Nuclear transport receptors in *A. nidulans*

Blast searches confirmed previous in silico analyses (Mans *et al.*, 2004; Espeso and Osmani, 2008) in which 17 loci coding for nuclear transporters were identified, as summarized in Table 1 (as indicated in this table, and for easy understanding of the text, we will refer hereafter to each *A. nidulans* locus with its designation and, in a superscript, the standard gene name in *S. cerevisiae*). Three genes encode for Ntf2-like family members (Table 1). NtfA (*An4942*) is a protein highly similar to *S. cerevisiae* and human nuclear transport factors Ntf2p and NTF2, respectively and is predictably involved in the nuclear import of the Ran-type GTPase RanA (*An5482*; Kadowaki *et al.*, 1994). Locus *An2737*, annotated as $mexA^{Mex67}$, encodes a protein with similarity to *S. cerevisiae* Mex67p and human nuclear RNA export factor 1, NXF1/TAP (Table 1). $MexA^{Mex67}$ predictably contains all of the characteristic domains described for its orthologues (reviewed in Conti and Izaurralde, 2001; Terry and Wente, 2009; and references therein): the RNA-binding and the leucine-rich repeat domains at the N-terminal part, and an NTF2-like domain and a UBA-like domain in the C-terminal region. The presence of these domains anticipates the interaction of $MexA^{Mex67}$ with NUPs and an NTF2-like export factor (Fribourg *et al.*, 2001; Grant *et al.*, 2003). Locus *An3864* encodes a putative homologue of the human NTF2-like export factor 1, p15/NXT1, and was designated as $nxtA^{p15}$. However, we were unable to identify a putative homologue for the *S. cerevisiae* essential mRNA transporter Mtr2p (Kadowaki *et al.*, 1994), which is a structural and functional homologue of NXT1 (Fribourg and Conti, 2003). Thus we predict the formation of a $MexA^{Mex67}$/$NxtA^{p15}$ heterocomplex in *A. nidulans* to mediate the export of specific mRNAs as occurs in higher eukaryotes (Zenklusen and Stutz, 2001).

A. nidulans locus/ systematic name[a]	*S. cerevisiae* // *H. sapiens* homologues % similarity/ identity *S.c.* vs. *A.n.* // *H.s.* vs. *A.n.*	Knockout functional analysis	Preferential cellular localization	
			At interphase	During mitosis
Ntf2-like family				
ntfA/AN4942 ntfA^{Ntf2}	Ntf2p // NTF2 77/59 // 59/41	Essential	Nuclear	nd
mexA/AN2737 mexA^{Mex67}	Mex67p // TAP-NXF1 49/30 // 44/23	Nonessential	Perinuclear	Total dispersion
No homologue	Mtr2p // –	—	—	—
nxtA/AN3864 ntxA^{p15} [b]	– // p15-NXT1 – // 47/27	Nonessential	Perinuclear	Total dispersion
Karyopherin-β superfamily				
kapA/AN2142 kapA^{Srp1}	Kap60p(Srp1p) // Imp-α 1-6 75/59 // 73/57	Essential	Nuclear	Partial dispersion (nuclear)
kapB/AN0906 kapB^{Kap95}	Kap95p(Rsl1p) // Imp β1 60/39 // 57/36	Essential	Perinuclear	Partial dispersion (NE)
kapC/AN0926 kapC^{Kap104}	Kap104p // Imp 2 51/30 // 56/35	Nonessential	Nuclear	Total dispersion
kapD/AN6006 kapD^{Nmd5}	Kap108p(Sxm1p) // Imp 7 45/26 // 46/27 Kap119p(Nmd5p) // Imp 8 47/28 // 46/27	Nonessential	Nucleocytoplasmic	Total dispersion
kapE/AN6591 kapE^{Cse1}	Kap109p(Cse1p) // CAS 61/41 // 55/36	Essential	Nuclear	Partial dispersion (nuclear)
kapF/AN6734 kapF^{Mtr10}	Kap111p(Mtr10p) // Trans-portin SR 52/31 // 44/26	Essential	Nuclear	Total dispersion
kapG/AN2164 kapG^{Kap114}	Kap114p(Hrc1004p) // Imp 9 38/22 // 42/24	Nonessential	Nucleocytoplasmic	Total dispersion
kapH/AN4053 kapH^{Kap120}	Kap120p(Lph2p) // Imp 11 48/27 // 48/28	Nonessential	Nucleocytoplasmic	Nuclear, mitotic spindle[c]
kapI/AN5717 kapI^{Pse1}	Kap121p(Pse1p) // Imp 5 59/39 // 57/35	Nonessential	Perinuclear	Nucleolus[c]
kapJ/AN2120 kapJ^{Kap123}	Kap123p(Yrb4p) // Imp 4 49/28 // 44/24	Nonessential	Nucleocytoplasmic	Nucleolus[c]
kapK/AN1401 kapK^{Crm1}	Kap124p(Crm1p) // Exp1/ Xpo1 73/54 // 71/54	Essential	Nuclear	Partial dispersion (nuclear)
kapL/AN3012 kapL^{Msn5}	Kap142p(Msn5p) // Exp 5 47/28 // 25/14	Nonessential	Nucleocytoplasmic	Total dispersion
kapM/AN8787 kapM^{Los1}	Los1p // Exp-T 45/24 // 45/25	Nonessential	Nuclear	Partial dispersion (nuclear)
kapN/AN7731 kapN^{Kap122}	Kap122p(Pdr6p) // Imp 13 26/14 // 41/21	Nonessential	Nucleocytoplasmic	Total dispersion

In addition to *S. cerevisiae* Mtr2p, no putative homologues were found in *A. nidulans* for human exportins 4 and 7, Ran-binding proteins 17 and 20, and Snurportin. *A.n.*, *A. nidulans*; *H.s.*, *H. sapiens*; *S.c.*, *S. cerevisiae*. Exp, exportin; Imp, importin, nd, not determined; –, nonexistent.

[a]Name adopted in this article indicating both *A. nidulans* and, in the superscript, the putative homologue in *S. cerevisiae* locus designations. For *S. cerevisiae* loci, the standard names at the *Saccharomyces* Genome Database (http//:www.yeastgenome.org) are used.

[b]In the absence of a *S. cerevisiae* NxtA homologue, the human homologue is indicated in the superscript.

[c]Transitory foci during mitosis.

TABLE 1: Nuclear transporters in *Aspergillus nidulans.*

Fourteen loci encode for proteins belonging to the karyopherin-β superfamily and consequently were designated as *kap* plus locus names from A to N. Among these nuclear receptors, KapD (encoded by locus *An6006*) was identified as the putative homologue of both *S. cerevisiae* Kap119p(Nmd5p) and Kap108p(Sxm1p) or human equivalents importins-7 and -8 (Table 1). A number of transporters

are absent from fungal genomes, suggesting their specificity in higher eukaryotes (indicated in Table 1; Espeso and Osmani, 2008). Additional in silico searches using Pfam domains related to this superfamily of proteins did not add more candidates to our predictions (Supplemental Figure S1).

The expression of these in silico–identified genes was confirmed by cDNA sequencing and the predicted amino acid sequences compared with those of automatic predictions at the database. Minor errors in intron predictions were found, and database entries were consequently modified. These corrections did not change the classification initially achieved. Thereafter, and with the aim to confirm these predictions, we generated a phylogenetic tree incorporating *Neurospora crassa*, *Schizosaccharomyces pombe*, *S. cerevisiae*, and *Homo sapiens* homologues (Supplemental Figure S1). In this tree, and in agreement with similarities in their sequences (Table 1), each *A. nidulans* Kap grouped well with its putative homologues. We then assumed similar functions for these transporters to those initially proposed for their homologues (reviewed in Terry and Wente, 2009). Three genuine exportins are predicted—KapK^{Crm1}, KapE^{Cse1}, and KapM^{Los1}—and nine importins—KapB^{Kap95}, KapC^{Kap104}, KapD^{Nmd5}, KapF^{Mtr10}, KapG^{Kap114}, KapH^{Kap120}, KapI^{Pse1}, KapJ^{Kap123}, and the importin-α homologue KapA^{Srp1}, acting as the importin-β1 adaptor. Finally, there are two candidates for mediators of bidirectional transport: KapN^{Kap122} and KapL^{Msn5}. Msn5p has been shown to have both importin and exportin activities in *S. cerevisiae* (Yoshida and Blobel, 2001). Although Kap122p is an importin in *S. cerevisiae* (Titov and Blobel, 1999;Terry and Wente, 2009), KapN^{Kap122} shares similarity with Imp13, a human bidirectional transporter (Mingot *et al*., 2001).

Functional analysis of nuclear transporters by generation of null alleles

To assess a role for these nuclear transporters in *A. nidulans*, we generated single-knockout mutants for each locus by means of a precise gene replacement procedure (see *Materials and Methods* and Supplemental Figure S2). The deletion of 11 of 17 transporters produced viable homokaryotic colonies in transformation experiments (Table 1, knockout functional analyses), demonstrating that these genes are not essential. *kapC^{Kap104}*, *kapD^{Nmd5}*, *kapG^{Kap114}*, *kapH^{Kap120}*, *kapJ^{Kap123}*, *kapL^{Msn5}*, *kapM^{Los1}*, and *kapN^{Kap122}* deletants showed a wild-type phenotype over a variety of culture conditions (different carbon or nitrogen sources, a range of temperatures, and in saline and/or osmotic stress; Supplemental Figure S3). Of interest, KapI^{Pse1} and MexA^{Mex67} constitute notable exceptions compared with their *S. cerevisiae* homologues, which are essential (for database see http://www.yeastgenome.org; Seedorf and Silver, 1997; Segref *et al*., 1997). *kapI^{Pse1}*- and *mexA^{Mex67}*-null strains grew in standard culture conditions but displayed morphological defects, such as reduced and compact growth and sparse conidiation (Figure 1A) (Etxebeste *et al*., 2009). Low (30°C) and elevated (42°C) temperatures affected colonial growth of both *kapI ^{Pse1}Δ* and *mexA^{Mex67}Δ* mutants but not the growth of other *kap*-null strains, such as *kapG ^{Kap114}Δ* (Figure 1A; see also Supplemental Figure S3). Considering NxtA^{p15} as a partner of MexA^{Mex67} activity, it is interesting to note that, in contrast to the morphological defect of *mexA^{Mex67}Δ* mutant, an *nxtA^{p15}*-null strain shows wild-type growth at standard culture conditions (37°C) but displays sensitivity to 42°C. All *nxtA^{p15}Δ mexA^{Mex67}Δ* and *mexA^{Mex67}Δ* strains showed a comparable thermosensitive phenotype and compact morphology at 37°C (Figure 1A), suggesting a major role of MexA^{Mex67} in the putative heteromer. A double-null *nxtA^{p15} mexA^{Mex67}* strain is viable and demonstrates the nonessentiality of a heteromeric NxtA^{p15}/MexA^{Mex67} transport pathway, but a compact colony morphology of the double-null mutant is observed in different growth conditions (Supplemental Figure S3), showing an additive effect of both null alleles. This additive phenotype suggests independent functions for each carrier (see also later discussion).

Homokaryotic transformants could not be obtained when deleting *kapE^{Cse1}*, *kapF^{Mtr10}*, *kapK^{Crm1}*, or *ntfA^{Ntf2}*, suggesting that these are essential genes. Consequently, transformants were maintained using the heterokaryon-rescue technique (Osmani *et al*., 2006b). Conidia from these heterokaryotic colonies were unable to grow on pyrimidine-selective solid medium (without supplementation of uracil and uridine; exemplified for *kapK^{Crm1}* knockout strains; Figure 1B), indicating the nonviability of those conidiospores bearing the null allele of the corresponding transporter. The presence of both recombinant and wild-type nuclei in the heterokaryotic mycelia was confirmed by PCR and Southern blot techniques (unpublished data). Thus we completed the list of indispensable transport pathways in *A. nidulans* by adding KapE^{Cse1}, KapF^{Mtr10}, KapK^{Crm1}, and NtfA^{Ntf2} to the previously identified essential nuclear carriers importin-β1, KapB^{Kap95} (Osmani *et al*., 2006a), and importin-α, KapA^{Srp1} (Araújo-Bazán *et al*., 2009).

We studied the germination process of mutant conidia to determine the effect of the deletion of these essential genes. Conidiospores from the isolated heterokaryons were cultivated in pyrimidine-selective liquid media at 37°C, where those conidia carrying the recombinant nucleus would grow to the extent that lack of the essential gene allows, and visualized after 24 and 72 h of incubation (Figure 1C). We observed isotropic growth and the establishment of polarity in conidia from *kapA^{Srp1}*-, *kapE^{Cse1}*-, *kapF^{Mtr10}*-, *kapK^{Crm1}*, and *ntfA^{Ntf2}*-null strains, but two main phenotypes were distinguished based on the number of nuclei present in the cell. In the first class, comprising *kapF^{Mtr10}Δ* and *kapA^{Srp1}Δ* mutants, a single nucleus per germling was observed after 4′,6-diamidino-2-phenylindole (DAPI) staining (n = 30 cells). This single nucleus was located in the proximity of the germinated conidium (Figure 1C, rows 2 and 3), suggesting a restricted nuclear mobility in these mutant backgrounds. The second class comprised *kapE^{Cse1Δ}*, *kapK^{Crm1Δ}*, and *ntfA^{Ntf2Δ}* mutant strains, in which two nuclei were observed and consequently the first mitosis occurred in the cells (n = 30; Figure 1C, rows 4– 6). In common for both classes, polar growth at initial stage of germination seemed not to be impeded, as germ tubes were observed emerging from most of conidia, but hyphal growth arrested, as major differences in length were not found between 24 and 72 h of culture. In addition, after 72 h of incubation, small DAPI-stained masses were found in some cells, indicating the existence of nuclear degradation or DNA missegregation. Overall, these results suggested a major role of KapA^{Srp1} and KapF^{Mtr10} in the onset of the first mitosis, whereas KapE^{Cse1}, KapK^{Crm1}, and NtfA^{Ntf2} are most probably required for completion of the first nuclear division. These transporters seem not to be required for the establishment of polarized growth, and the inhibition in apical extension observed might be triggered as a consequence of this mitotic block or as general failure of a number of cellular processes (e.g., blockage of transcription factor import/export, mRNA cytoplasmic transport). This and previous work (Osmani *et al*., 2006a) show that the null *kapB^{Kap95}* strain displays the most extreme degree of developmental affection, since conidia germinated, but neither polar growth nor mitosis was observed (Osmani *et al*., 2006a), supporting, thus, a key role of KapB^{Kap95} in both cellular processes.

Cellular distribution of nuclear transporters during interphase

A noteworthy issue to resolve was the localization of the nuclear transportome in a multinucleated vegetative cell. With this aim we

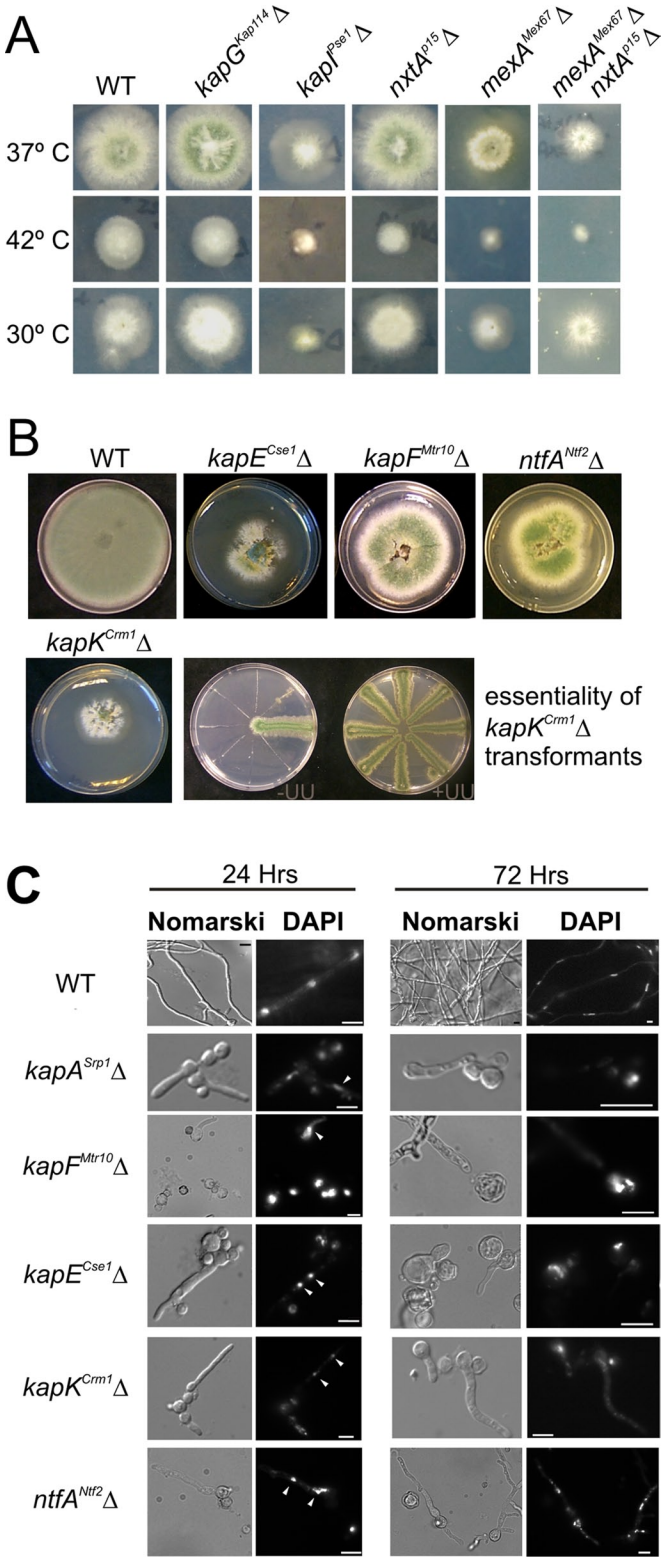

FIGURE 1: Null mutants in nuclear transporters displaying morphological defects or that are essential. (A) Morphological alterations caused by the deletion of nonessential KapI^{Pse1} and MexA^{Mex67}/NxtA^{p15} transporters. Strains MAD2159, MAD2332, MAD3017, and MAD3281 were cultured at different temperatures and colony radial growth compared with that measured at 37°C with the wild-type strain (MAD1425). A *kapG*$^{Kap114}\Delta$-null mutant (MAD2158) was included as a reference because its shows the wild-type phenotype generated after the deletion of most nonessential karyopherins (see text). (B) Heterokaryotic colony morphology caused by the deletion of essential nuclear transporters KapE^{Cse1}, KapF^{Mtr10}, KapK^{Crm1}, and NtfA^{Ntf2}. The heterokaryon rescue technique allows propagation of *kapE*^{Cse1}-, *kapF*^{Mtr10}-, *kapK*^{Crm1}-, and *ntfA*^{Ntf2}-null mutant strains as heterokaryons and phenotypic analysis of null conidia from these heterokaryotic colonies, as parental conidia do not grow on selective media lacking pyrimidines (uracil and uridine [UU]). As a representative example, the *kapK*$^{Crm1}\Delta$ growth test is shown (inset with colonies inoculated in a radial distribution). The absence of growth onto the selective media (−UU) demonstrates the lethal phenotype of the deletion allele. (C) Microscopic growth analysis of germinating conidia from mutants in essential transport pathways. Conidia from the heterokaryons were incubated in selective media for 24 and 72 h at 37°C. Germ-tube generation was analyzed, and the number of nuclei and their locations and morphology were determined using DAPI staining. Scale bars, 5 μm.

systematically generated strains expressing fluorescent-tagged versions of nuclear carriers (see *Materials and Methods* for details and Supplemental Figure S2). Strains expressing C-terminally green fluorescent protein (GFP)–tagged versions of KapC^{Kap104}, KapD^{Nmd5}, KapG^{Kap114}, KapH^{Kap120}, KapL^{Msn5}, KapM^{Los1}, and KapN^{Kap122} transporters lacked any appreciable phenotype. However, exceptions were those strains expressing NtfA^{Ntf2}::GFP or KapJ^{Kap123}::GFP. The former displayed a heterokaryotic development similar to the null *ntfA*^{Ntf2} strain, so we concluded that GFP tagging rendered a nonfunctional NtfA^{Ntf2} protein. Therefore further characterization of NtfA^{Ntf2}::GFP also required the heterokaryon-rescue technique. Strains expressing KapJ^{Kap123}::GFP showed limited growth on minimal compared with complete media, especially when incubation temperature was 30°C (Supplemental Figure S4A). It is worth noting that in *S. cerevisiae* the *kap123*Δ allele causes a reduced growth rate in complete medium (Rout *et al.*, 1997). However, this is not the case for a *kapJ*$^{Kap123}\Delta$ mutant. In minimal medium, DAPI staining of *kapJ*^{Kap123}*::gfp* cells revealed an anomalous distribution of DNA in nuclei, suggesting that C-terminal GFP tagging of KapJ^{Kap123} might cause missegregation of DNA, perhaps causing the restricted-growth phenotype observed (Supplemental Figure S4C). Then we generated a GFP::KapJ^{Kap123} strain (MAD3563), which showed a wild-type phenotype, and therefore it was used for subsequent localization analyses.

Expression of full-length chimeras was verified by Western blot assays, in which most of them showed the expected mobility according to their molecular weights (Supplemental Figure S5). However, KapF^{Mtr10}::GFP showed a markedly lower mobility, and KapL^{Msn5}::GFP displayed a pattern of four bands, which suggests the existence of either alternative forms or posttranslational modifications in this transporter. Detection of MexA^{Mex67}::GFP was always poor, but a band of the expected size was visualized (Supplemental Figure S5).

For localization studies special care was taken to image cells with at least four or five nuclei in either apical or subapical compartments. When fluorescence was low or nuclear fluorescence could not be easily differentiated from the cytoplasmic background, we constructed strains coexpressing the GFP-tagged transporter and the histone H1 (HhoA) fused to mCherry (mCh; Cherry red) as a nuclear marker. Prior to further analyses, we verified that the nuclear transporter chimeras displayed the same localization in wild-type and *hhoA::mCh* genetic backgrounds.

Three categories were differentiated according to their distribution patterns in interphase (Figure 2). The first group comprised KAPs having a preferential nuclear localization, with a ratio of nuclear/cytoplasmic fluorescence greater than three (Figure 2A). This

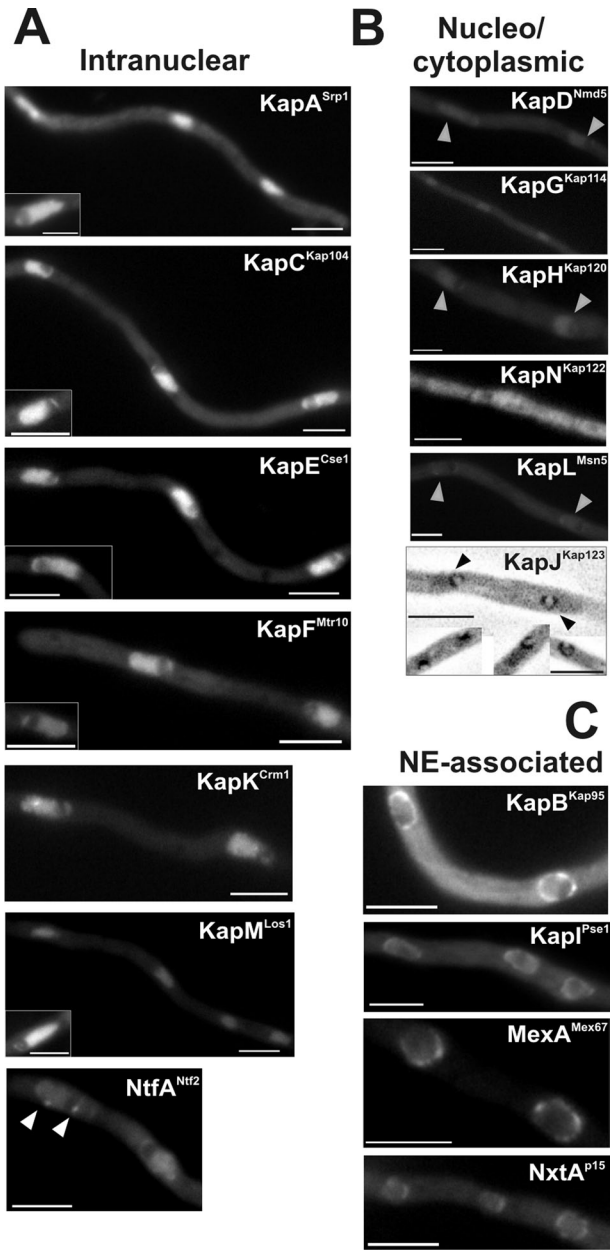

FIGURE 2: Distribution of nuclear transporters during interphase. nuclear transporters were classified into three groups: (A) those showing an intranuclear localization, (B) those displaying a nucleocytoplasmic localization, and (C) those with preferential perinuclear or NE-associated localization. In the insets, magnifications of nuclei exemplify the absence of fluorescence at nucleoli, which was confirmed by the observation of the nucleolar protein An-Fib. For KapJ^{Kap123}, a maximal intensity projection of deconvolved z-stacks in an inverted display shows the localization of GFP::KapJ^{Kap123} in the proximity of nucleoli. See the text for arrowhead explanation. Homokaryotic strains used here: MAD2067, MAD2913, MAD2161, MAD2162, MAD2163, MAD2164, MAD2165, MAD2175, MAD2325, MAD2914, MAD2652, MAD2328, MAD2331, MAD2330, MAD2333, and MAD3563. Scale bars, 5 μm.

group included KapA^{Srp1}, KapC^{Kap104} KapE^{Cse1}, KapF^{Mtr10}, KapK^{Crm1}, and KapM^{Los1}. Although NtfA^{Ntf2}::GFP fusion was not functional, we determined its localization in heterokaryotic cells in which at least two mitoses occurred. NtfA^{Ntf2} accumulated in the nucleus and at foci close to the nuclear periphery, probably near the NE (visualized in 90% of nuclei; n = 20; Figure 2A, white arrowheads). The seven transporters belonging to this group presented a regular distribution at the nucleoplasm but showed no fluorescence at the nucleolus, as observed in colocalization studies with the mCh-tagged nucleolar protein fibrillarin, An-Fib (AN0745.3; Ukil *et al*., 2009). See Supplementary Figure S6, for the KapK^{Crm1}::GFP chimera.

Those KAPs showing a ratio of nuclear versus cytoplasmic fluorescence less than three were designated as "nucleocytoplasmic" karyopherins. The fusion proteins included in this second group were C-terminally GFP-tagged KapD^{Nmd5}, KapG^{Kap114}, KapH^{Kap120}, KapN^{Kap122},and KapL^{Msn5} and GFP::KapJ^{Kap123} (Figure 2B; KapJ^{Kap123}::GFP is shown in Supplemental Figure S4, B and C). None of the transporters was excluded from nuclei, and nuclear fluorescence from tagged KAPs was always visible (gray arrowheads indicate nuclei positions using HhoA::mCh; Figure 2B). Both GFP/KapJ^{Kap123} chimeras presented a similar distribution at the periphery of the nucleolus (Figure 2B and Supplemental Figure S4B) and as demonstrated colocalization with An-Fib-mCh (shown for GFP::KapJ^{Kap123} in Supplemental Figure S6). In the cytoplasm, fluorescence distribution along the hypha was homogeneous for all chimeras, with the major exception of KapN^{Kap122}::GFP, which showed a speckled distribution (Figure 2B and Supplemental Figure S4D).

The C-terminally GFP-tagged versions of KapB^{Kap95}, KapI^{Pse1}, MexA^{Mex67}, and NxtA^{p15} constitute the third group, termed "NE-associated" transporters (Figure 2C). These transporters showed an accumulation at the nuclear periphery similar to that observed for nucleoporins (Figure 2C; Osmani *et al*., 2006a), and KapB^{Kap95} also accumulated in the proximity of the spindle pole body (SPB), the fungal centrosome, as indicated by colocalization with Nud1-mCh (unpublished data; see later discussion for the use of this SPB marker). Of note, localization of NxtA^{p15} at the NE depends on MexA^{Mex67}, since dispersion along the cytoplasm and nuclei was observed for NxtA^{p15}::GFP in a null *mexA*^{Mex67} background (unpublished data; strain MAD3282). As for the rest of transporters, these are also excluded from nucleolus (exemplified for KapB^{Kap95} in Supplemental Figure S6).

In view of the absence of predicted transmembrane domains in these nuclear carriers, it is reasonable to presume direct or mediated contacts with the constituents of the NPC. Although has not been investigated further, the study of the localization of nuclear carriers during mitosis suggests a dependence of the so-called "soluble-transport" machinery on the active transport and full assembly of NPCs.

Distribution of nuclear transporters during mitosis

Mitosis in *A. nidulans* has been defined as partially opened (De Souza and Osmani, 2007) because partial disassembly of the NPC during mitosis modifies the permeability of the NE, allowing mixing of nuclear and cytoplasmic proteins. Predictably, nuclear transporters may alter their localizations following mitotic FG-nucleoporin reallocations.

We excluded from this study those strains expressing KapJ^{Kap123}::GFP or NtfA^{Ntf2}::GFP, due to the functional deficiency caused by the fluorescent tag. A general observation for all tested constructs is that nuclear fluorescence was reduced when nuclei entered mitosis. In this context, we classified the nuclear transporters into three groups. Figure 3 shows those transporters that displayed dispersion of fluorescence between nucleus and cytoplasm during mitosis (see also the associated videos: KapC^{Kap104}::GFP (Supplemental Video S3), KapD^{Nmd5}::GFP (Supplemental Video S4), KapF^{Mtr10}::GFP (Supplemental Video S6), KapG^{Kap114}::GFP

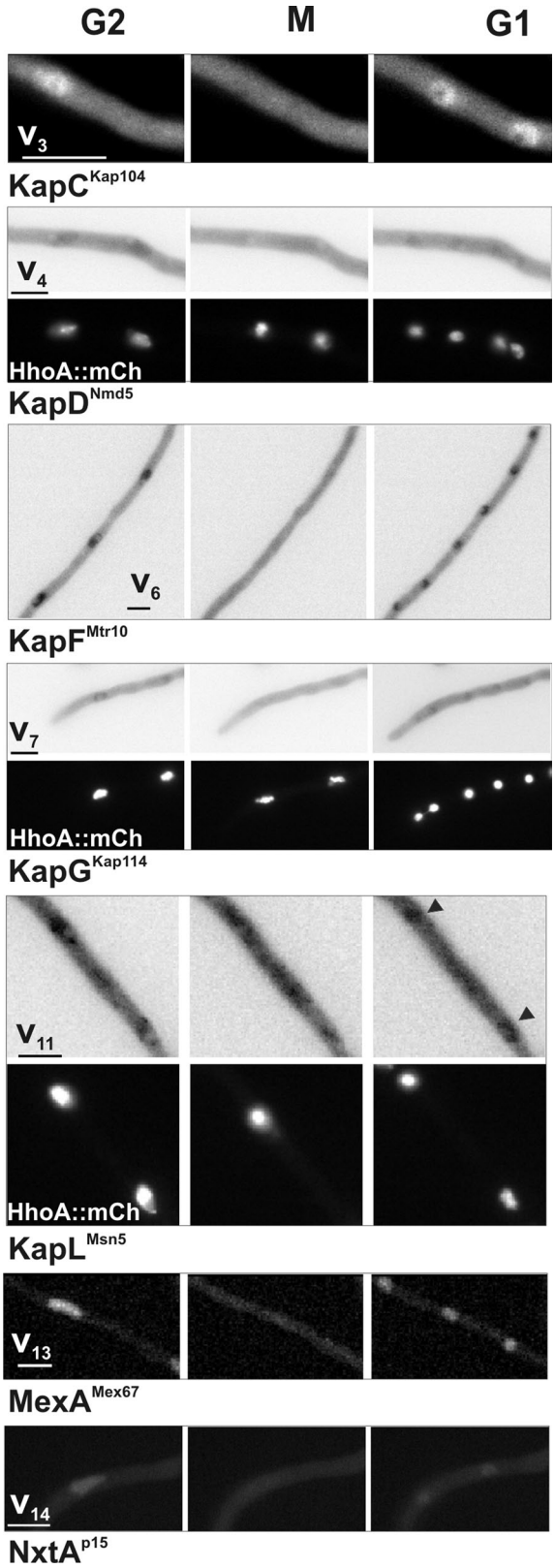

FIGURE 3: Nuclear transporters showing total dispersion during mitosis. Seven of the nuclear transporters displayed cytoplasmic dispersion from their interphasic localizations during mitosis. Selected frames and regions from videos (Supplemental Videos S3, S4, S6, S7, S11, S13, and S14) of representative cells at late G2, mitosis (M), and early G1 stages are shown. In the case of carriers with nucleocytoplasmic localization, KapD^{Nmd5}, KapG^{Kap114}, and KapL^{Msn5}, nuclei were visualized during cell cycle using mCherry-tagged histone H1 (HhoA::mCh) as a nuclear marker (strains MAD2853, MAD2854, and MAD2653, respectively). Scale bars, 5 μm.

(Supplemental Video S7), KapL^{Msn5}::GFP (Supplemental Video S11), MexA^{Mex67}::GFP (Supplemental Video S13), and NxtA^{p15}::GFP (Supplemental Video S14). For nucleocytoplasmic transporters, mitosis was followed by colocalization with HhoA::mCh (Figure 3).

The second group included KapA^{Srp1}::GFP (Supplemental Video S1), KapE^{Cse1} (Supplemental Video S5), and KapM^{Los1} (Supplemental Video S12), which showed partial dispersion during mitosis (Figure 4A). The intensity of nuclear florescence during mitosis decreased in these cases but was not completely dispersed into the cytoplasm. This indicates that a pool of these transporters may remain inside the nucleus, interacting with or attached to nuclear structures or protein complexes. KapK^{Crm1} and more dramatically KapB^{Kap95} were partially retained in the nucleoplasm and at the nuclear envelope, respectively (Supplemental Videos S10 and S2, respectively). In particular, KapB^{Kap95}::GFP allowed the tracking of the NE during mitosis and the visualization of its rupture to render independent daughter nuclei (Figure 4A, blue arrowheads at KapB^{Kap95} insets). This observation indicated a possible close relationship between KapB^{Kap95} and core nucleoporins of the mitotic NPC. We were able to observe the compartment that contains the nucleolus during mitosis when either KapB^{Kap95} or KapK^{Crm1} was monitored (Figure 4A, white arrowheads in either KapB or KapK). KapK^{Crm1} briefly remains at the nucleoplasm bordering the cytoplasmic parental nucleolus before it starts disassembling. An-Fib exits the parental nucleolus after the migration of KapK (Supplemental Video S16 and kymograph in Figure 4B). The maintenance of these two KAPs in close relationship with the nucleus or NE during the mitotic process suggests roles in mitotic progression and/or restart of nuclear transport after NPC rearrangement.

The last group includes KapH^{Kap120}::GFP, KapI^{Pse1}::GFP, and GFP::KapJ^{Kap123}, which are KAPs showing specific locations during mitosis (Figures 5 and 6; see next sections).

KapH^{Kap120} locates at the mitotic spindle

The start of chromatin condensation in prophase coincided with an aggregation of KapH^{Kap120} fluorescence in a spot that continued stretching out in a shape resembling that of the mitotic spindle (Figure 5A, black arrowhead, and Supplemental Video S8). After mitosis KapH^{Kap120} was redistributed into daughter nuclei. A possible association with the mitotic spindle could not be verified using the available GFP-tagged version of tubulin α, *tubA*, because of instability of the KapH^{Kap120}::mCh protein. Consequently, we visualized the position of the SPB using the Nud1::mCh fusion as a marker. We verified that, at the onset of mitosis, KapH^{Kap120} starts to accumulate at the proximity of the SPBs prior to their separation (see mitosis for selected nucleus 1, n1, in Figure 5B). Then the fluorescence accumulation of KapH^{Kap120}::GFP elongated as daughter SPBs moved and mitosis proceeded (Figure 5B, n1 and n2 mitoses, and Supplemental Video S17). After mitotic completion, KapH^{Kap120}::GFP fluorescence dispersed and in late G1 recovered the nucleocytoplasmic location described during interphase. The nuclear reporter StuA-NLS-DsRed requires an active nuclear import system to accumulate in the nucleus. The cytoplasmic localization of this reporter when KapH^{Kap120} locates at the mitotic spindle demonstrates that this occurs in the absence of a functional NPC (Figure 5C).

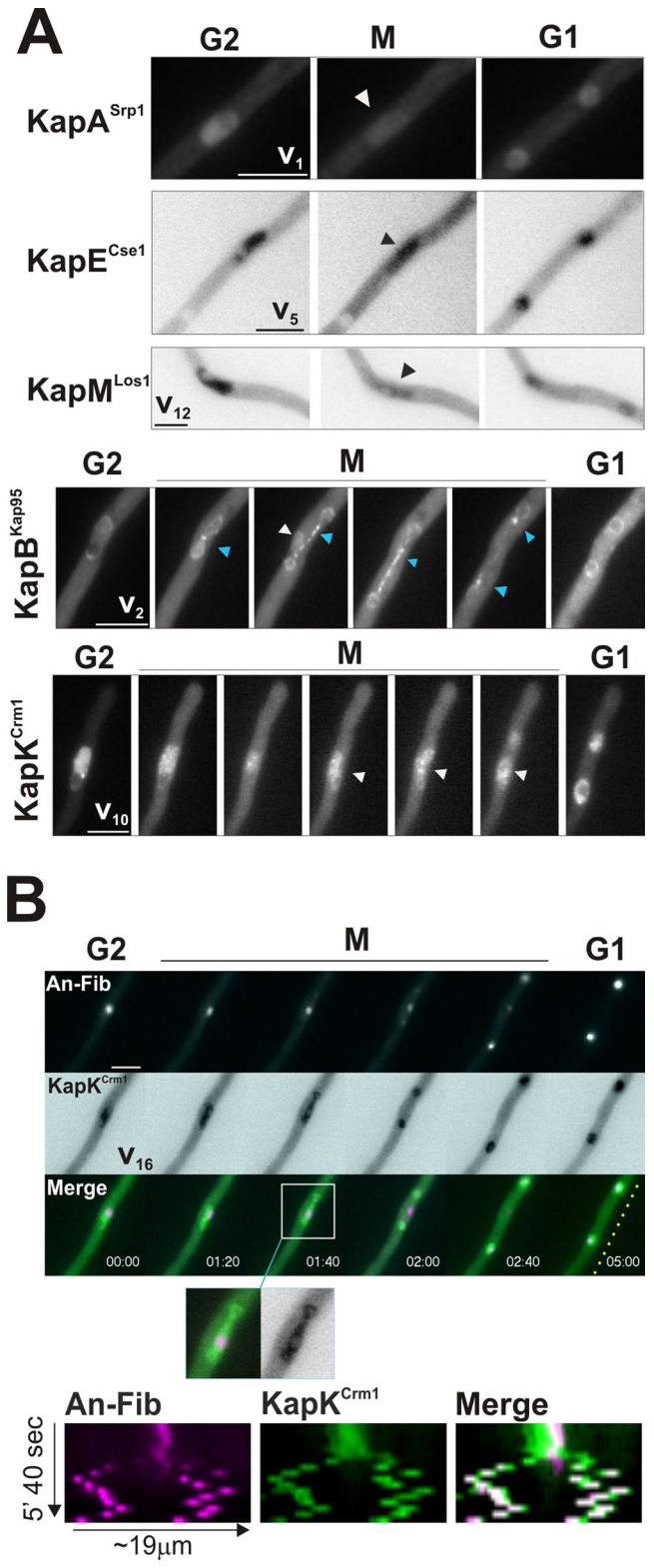

FIGURE 4: Nuclear transporters displaying partial dispersion during mitosis. (A). As in Figure 3, selected frames and regions from videos (Supplemental Videos S1, S2, S5, S10, and S12) of representative cells at late G2, mitosis (M), and early G1 stages are shown for five KAPs. The fluorescence signal redistributes at the onset of mitosis and in G1 recovers its interphasic localization. Nuclear fluorescence is seen for KapA^{Srp1}, KapE^{Cse1}, and KapM^{Los1}, showing the last two insets in inverted display for best visualization. At early mitosis KapB^{Kap95} and KapK^{Crm1} disperse but some remains in the mitotic nucleus, being associated with the NE (white arrowheads). (B) KapK^{Crm1} (Supplemental Video S16; strain MAD3540; KapK^{Crm1}-GFP, green) remains nuclear during mitosis. KapK^{Crm1} is excluded from the parental nucleolus during the mitotic process. Magnification of a nucleus at early mitosis shows how KapK^{Crm1}::GFP fluorescence is distributed uniformly along the nucleoplasm but excluded from the nucleolus, as shown by colocalization with fibrillarin (An-Fib, magenta). A kymograph of this series of images, along the cell region indicated by the yellow dotted line, illustrates the absence of KapK^{Crm1} from the nucleolus during the process, but especially when the nucleolus is extruded and starts its disassembly. Time scale, min:s. Scale bars, 5 µm.

KapI^{Pse1} and KapJ^{Kap123} locate at the mitotic nucleolus

KapI^{Pse1} and KapJ^{Kap123} display different locations at interphase, but during mitosis both KAPs are localized in the nucleolus. KapI^{Pse1} disperses from the NE, and we noticed a temporary and precise accumulation during mitosis that did not coincide with either of the daughter nuclei but was situated between them after DNA segregation (Supplemental Figure S7 and Supplemental Videos S9 and S19). Colocalization with the nucleolar An-Fib-mCh protein confirmed that such compartment was the nucleolus (Figure 6A and Supplemental Video S18). KapI^{Pse1} accumulates at the parental nucleolus prior to the exit of An-Fib and lasts until the completion of An-Fib incorporation into daughter nucleoli (Figure 6A and Supplemental Video S18).

KapJ^{Kap123}, initially at the border of the nucleolus, disperses momentarily at the onset of mitosis and then begins to accumulate in the cytoplasmic parental nucleolus (Figure 6B and Supplemental Video S20). KapJ^{Kap123} localization, as seen for KapI^{Pse1}, coincided with the process of nucleolar dispersion of An-Fib and the de novo formation of daughter nucleoli. Figure 6C shows that active nuclear transport recovered in daughter nuclei when both KapI^{Pse1} and KapJ^{Kap123} accumulated in the parental nucleolus (Figure 6C, red arrowheads, M/G1 phase). We did not observe a preferential localization within the daughter nucleoli, suggesting that these KAPs might be specifically directed into the compartments that contain the nucleoli and be involved in their disassembly and the recycling of components to the new nucleoli but not directly in their reassembly at nucleolar organizing regions. Because null *kapJ*^{Kap123} and *kapI*^{Pse1} are viable, a functional redundancy might be proposed in *A. nidulans* for these two KAPs, as previously described in *S. cerevisiae* (Rout *et al.*, 1997).

DISCUSSION

The first systematic characterization of the nuclear transport machinery in a filamentous fungus highlights several interesting issues relevant to the understanding of this key regulatory process in multinucleated cells. Fluorescent tagging and deletion analysis has permitted us to define the cell cycle–specific KAP distribution map and to determine the four essential nuclear transport pathways in *A. nidulans*. The general import pathway comprises the importin α/β1 heterodimer, KapA^{Srp1}/KapB^{Kap95}, and KapE^{Cse1}, which must be the specific importin-α exporter required for cytoplasmic recycling of this adapter. KapK^{Crm1}/CrmA mediates the general nuclear export pathway (Todd *et al.*, 2005; Bernreiter *et al.*, 2007). KapF^{Mtr10}, a transportin SR, is predicted to export diverse mRNAs and other ribonucleoproteins (Senger *et al.*, 1998; Murthi *et al.*, 2010). Finally, NtfA^{Ntf2} is the key carrier that might import the Ran GTPase, RanA, an indispensable element for obtaining the energy and transport directionality across the NPC.

Information about the NtfA^{Ntf2}–RanA relationship is limited due to the inability to obtain functional fluorescent fusions. However, conditional mutations in both general import and export systems

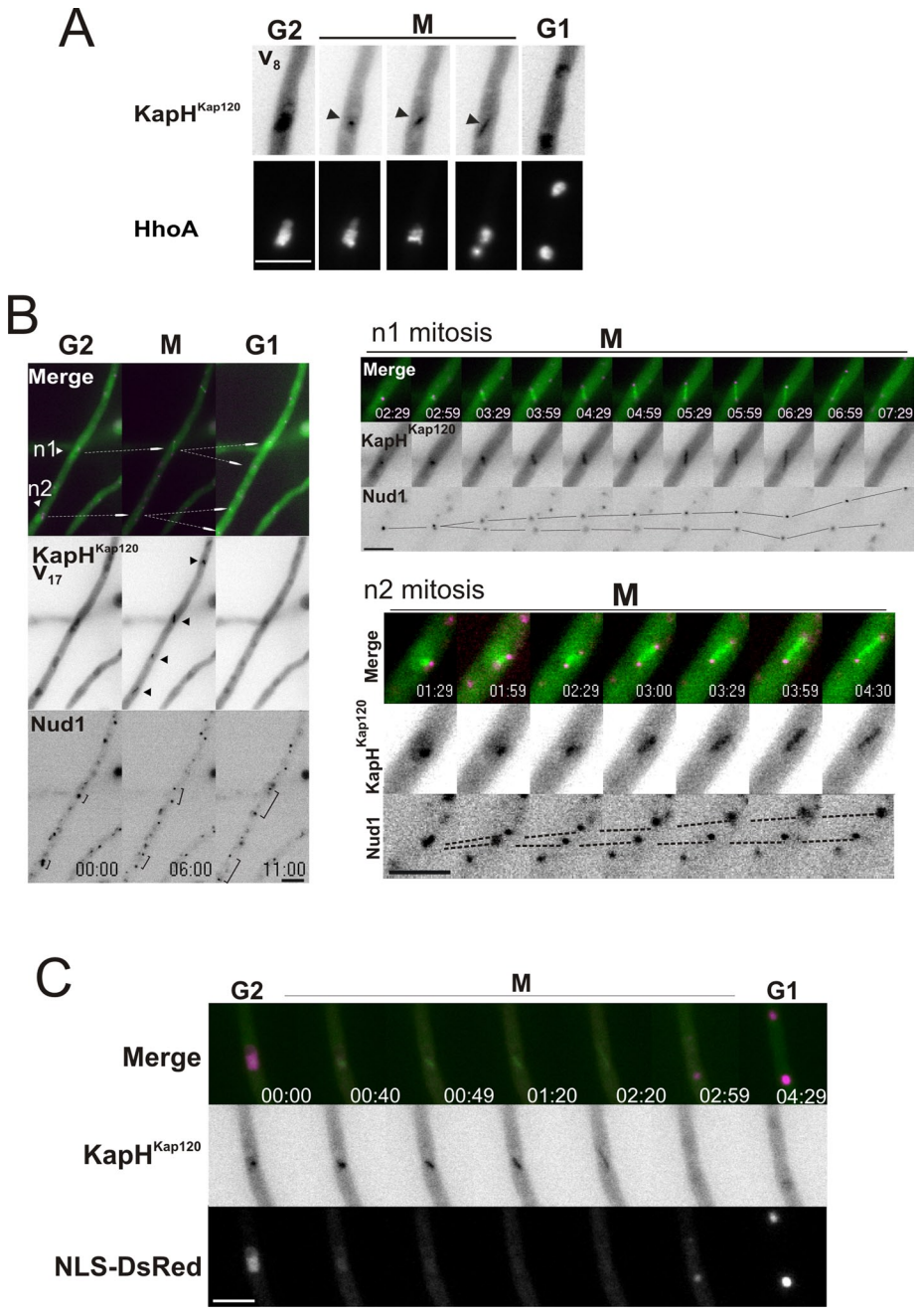

FIGURE 5: KapH^{Kap120} locates at the mitotic spindle. (A) KapH^{Kap120} disperses from its nuclear localization at G2 and accumulates in a dot at the onset of mitosis, when chromatin starts to condense (visualized using HhoA-mCh; Supplemental Video S8; strain MAD2855), and the signal for KapH^{Kap120} fluorescence elongates (black arrowheads) during mitosis, then concentrating again in daughter nuclei at G1. (B) Selected images from Supplemental Video S17 show the simultaneous visualization of KapH^{Kap120}::GFP (green) and the SPB protein Nud1 (Nud1-mCh, magenta) in cells from strain MAD3564. Arrows follow divisions of nuclei n1 and n2, which are shown in more detail on the right. Trajectories of SPBs, labeled with Nud1, are followed with a line. (C) Time-lapse images from a MAD3772 strain cell showing the localization of KapH^{Kap120} during the cytoplasmic dispersion of NLS-DsRed reporter at mitosis. Time scale, min:s. Scale bars, 5 μm.

previously allowed the identification of different cargoes and demonstrated their conserved mechanisms. The transcription factor (TF) for nitrate assimilation, NirA, and the regulator of nitrogen metabolism, AreA, are cargoes of the exportin KapK^{Crm1} (Bernreiter *et al.*, 2007; Todd *et al.*, 2005). Import of VeA, the developmental regulator in response to light, requires the importin-α/β1 heteromer (Araújo-Bazán *et al.*, 2009). Importin-α acts as the only known adaptor of importin-β1 in *A. nidulans* and recognizes monopartite and bipartite NLSs (Fernandez-Martinez *et al.*, 2003; Stinnett *et al.*, 2007; Araújo-Bazán *et al.*, 2009). However, VelB is an example of an alternative import mechanism through the importin-α/β1 pathway, since, lacking an obvious NLS, it is transported into the nucleus via interaction with VeA (Bayram *et al.*, 2008).

Of interest, deletion of *kapI*^{Pse1} and *mexA*^{Mex67} genes does not cause lethality in *A. nidulans*, whereas in *S. cerevisiae* both Kap121p/Pse1p and Mex67p are essential transporters. KapI^{Pse1} activity is likely to mediate the import of key factors during the development of asexual reproductive structures (Etxebeste *et al.*, 2009). The MexA^{Mex67}/NxtA^{p15} putative heterodimer is predicted to mediate specific mRNA export (Zenklusen and Stutz, 2001). Single- or double-null mutants do not cause lethality, although the morphological defects of the *mexA*^{Mex67}Δ strain and the mislocalization of NxtA^{p15} in this mutant background demonstrate that MexA^{Mex67} is the principal component of this pathway in *Aspergillus*.

From a total of 14 predicted transport pathways, we have not found experimental evidence for roles for eight of them. Sensitivity to an elevated salt concentration and sensitivity to alkalinity are phenotypes derived from loss-of-function mutations in the pH regulator PacC (Peñalva *et al.*, 2008) or the cation stress response TFs SltA and CrzA (Spielvogel *et al.*, 2008). Although PacC localizes into the nucleus in an importin-α–independent manner (Fernandez-Martinez *et al.*, 2003), none of the viable *kap*Δ strains displayed a defect on pH regulation. In *S. cerevisiae* Crz1p is imported by Nmd5p, being homologues of CrzA and KapD^{Nmd5}, respectively. Both Crz1p and Nmd5p nulls show similar phenotypes (Polizotto and Cyert, 2001). However, neither *kapD*^{Nmd5}Δ nor any other *kap*Δ strains showed calcium or cation sensitivity comparable to that shown by *crzA*Δ or *sltA*Δ mutants (Spielvogel *et al.*, 2008). These data strongly support redundant roles of nuclear transporters in a variety of shuttle mechanisms, as previously proposed for other organisms (Fiserova and Goldberg, 2010).

The regular distribution of all nuclear carriers during interphase supports a model of transport organization in which every nucleus within the syncytium possess the required elements to mediate active transport. Proof of this are those cargoes that are coordinately transported in all nuclei, such as CrzA, NirA, NapA, PacC, or VeA (Bernreiter *et al.*, 2007; Araújo-Bazán *et al.*, 2008, 2009; Peñalva *et al.*, 2008; Spielvogel *et al.*, 2008). However, one exception is FlbB, the bZIP-type factor

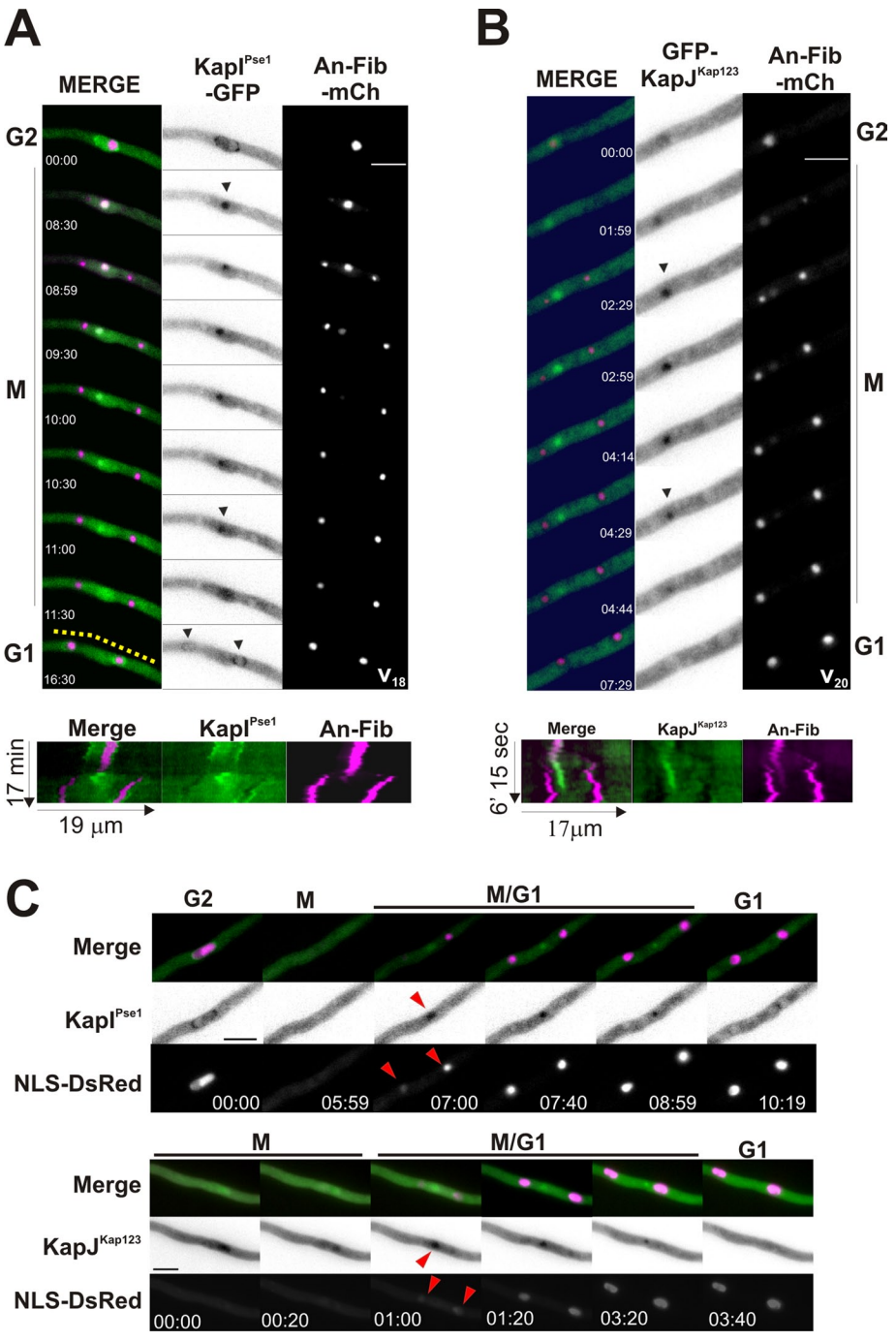

FIGURE 6: KapJ^{Kap123} and KapI^{Pse1} localizations are linked to the mitotic nucleolus. (A) KapI^{Pse1} nucleolar accumulation coincides with initiation of An-Fib migration to daughter nuclei (right, Supplemental Video S18, strain MAD3539). A kymograph illustrates the colocalization of KapI^{Pse1}::GFP (green) and An-Fib-mCh (magenta) in the mitotic nucleolus but not in daughter nucleoli, where KapI^{Pse1} localizes at the NE, as in an interphase parental nucleus (left, bottom). (B) KapJ^{Kap123}, GFP::KapJ^{Kap123} is shown (strain MAD3594), which shows a perinucleolar localization and first disperses but rapidly starts to accumulate in the nucleolus. As previously described for KapI^{Pse1}, KapJ^{Kap123} (GFP-KapJ^{Kap123}, green, Supplemental Video S20) localizes to the mitotic nucleolus during the process of fibrillarin segregation to daughter nuclei (An-Fib-mCh, magenta). When An-Fib relocation is completed, KapJ^{Kap123} accumulates to the new nucleolar peripheries again. Kymograph at the bottom shows that both KapJ^{Kap123} and An-Fib colocalized during most of the mitotic process, but KapJ^{Kap123} remains in the parental nucleolus until complete relocation of An-Fib. Time scale, min:s. Kymographs were done along the yellow dotted lines indicated at respective inserts. (C) Accumulation of KapI^{Pse1} and KapJ^{Kap123} in the parental nucleolus coincides with recovery of active nuclear transport, as shown by nuclear accumulation of NLS-DsRed reporter at the M/G1 transition (indicated with red arrowheads, strains MAD3771 and MAD3817). Scale bars, 5 µm.

modulating asexual development, which shows preferential accumulation at the most apical nucleus (Etxebeste *et al.*, 2008). This finding predicts the presence of transport mechanisms that might discriminate among different cargoes and specifically shuttle them into all or selected nuclei.

Changes in the subcellular distribution of nuclear carriers during mitosis offered an avenue for delimiting the processes in which these proteins are involved. The partial disassembly of NPCs changes the localization of several nuclear transporters. Such changes hint at how key processes in the mitotic nucleus might occur. Mitotic dispersion of transportin-SR KapF^{Mtr10} and the NE-associated MexA^{Mex67}/NxtA^{p15} heterocomplex add support to early conclusions that RNA export must be low or practically nonexistent during mitosis (Espeso and Osmani, 2008). However, mechanistically, Mex homologues are expected to interact with the Nup84 subcomplex (Yao *et al.*, 2008), which in *A. nidulans* is part of the mitotic NPC core structure (Osmani *et al.*, 2006a); thus the existence of specific mechanisms, that is, posttranslational modifications, acting on MexA^{Mex67} has to be postulated. Interesting regulatory or interaction events might occur during the mitotic localization of KapH^{Kap120} following tubulin assembly at the mitotic spindle. This observation suggests a function for this transporter during or after spindle assembly. It is tempting to suggest a role in the transport of spindle-associated proteins, tubulin itself, or with chromosomes, that is, at the kinetochores, as has been shown for other carriers (Kalab and Heald, 2008, and references therein). A characterization of the spindle composition in *S. cerevisiae* showed the interaction of Kap120p with Mtw1p, an essential component of the MIND kinetochore complex (Wong *et al.*, 2007). Finally, the nucleolar localizations of both KapI^{Pse1} and KapJ^{Kap123} during mitosis link these transporters with the process of nucleolar division, hypothetically as an extension of their putative interphase roles in the transport of ribosomal components (Sydorskyy *et al.*, 2003). However, *kapH^{Kap120}*, *kapI^{Pse1}* and *kapJ^{Kap123}*, deletions are not lethal, suggesting that the presence of redundant roles is one open possibility in *A. nidulans*.

KapB^{Kap95} and KapK^{Crm1} are essential karyopherins associated with mitotic nuclei. In addition to their predicted and demonstrated roles in general import and export pathways, we postulate that permanence of KapB^{Kap95} and KapK^{Crm1} at the nucleus during mitosis indicates that they have important postmitotic functions, for instance, in a primary step at the restart of nuclear

transport after NPC reassembly, rendering proper distribution of key factors such as Ran-GAP after its unspecific nuclear entry in mitosis (De Souza *et al.*, 2004). These transporters could also participate in proper distribution of cell-cycle regulatory proteins during interphase and after mitosis because conidium germination and the first mitosis are affected in *kapK*^{Crm1} and, more severely, in *kapB*^{Kap95} deletants (Osmani *et al.*, 2006a; this work). As described for Kap95p or Kap95p/Srp1p heterocomplexes in *S. cerevisiae* (Taberner and Igual, 2010), KapB^{Kap95} could be involved in the import of transcriptional factors required at *Start* of which down-regulation causes cell cycle arrest.

This work brings together the localization and functionality of nuclear carriers with previous systematic studies in the organization of NPC at interphase and mitosis. The battery of nuclear carriers in *A. nidulans* suggests conserved transport pathways between high and low eukaryotes. However, an interesting biological question to address in the future is how these general mechanisms have been adapted to serve a coenocytical lifestyle. Future studies will focus on understanding how cargoes and carriers overcome the long cellular distances in filamentous fungal cells to coordinately respond to ambient and internal stimuli.

MATERIALS AND METHODS

Strains, media, and culture conditions

Media and general techniques for *A. nidulans* culture and transformation were used as previously described (Araújo-Bazán *et al.*, 2008). *A. nidulans* strains used in this study carried markers in standard use (Clutterbuck, 1993) and are listed in Supplemental Table S1. Strain TN02A3 (Nayak *et al.*, 2006), identified here as MAD1425, was used for the systematic deletion and fluorescent tagging of nuclear transporters. MAD1427 was used for the generation of double-null *mexA*^{Mex67}/*nxtA*^{p15} and *mexA*^{Mex67}Δ/*gfp*-tagged *nxtA*^{p15} strains. Strain MAD2484 was used as recipient for colocalization studies of GFP- tagged Kaps and the SPB protein Nud1 and strain AY02 for colocalization studies with the active-nuclear-transport marker NLS-DsRed. Strains carrying deletions in essential genes were handled as heterokaryons ("heterokaryon rescue technique") and, hence, propagated by transfer of mycelia pads (Osmani *et al.*, 2006b). Phenotypes caused by the deletion of purportedly nonessential genes were studied under a range of ambient stresses. Salt or osmotic stress was induced by addition of $CaCl_2$ (0.1 M), $MgCl_2$ (0.1 M), LiCl (0.1, 0.3M), NaCl (0.1, 1 M), or KCl (0.1 M). Acidic or alkaline stress was induced adjusting media pH to 5.2 or 8.0 with NaH_2PO_4 (0.1 M) or Na_2HPO_4 (0.1 M), respectively. Temperature effects were studied by comparing phenotypes at 30 and 42°C to those at 37°C. Radial extension of mutant strains was always compared with that of the parental MAD1425 strain.

Bioinformatic tools

Amino acid sequences of previously identified yeast (*S. cerevisiae*) and human transporters were used to search for *A. nidulans* putative homologues using BLASTp and tBLASTn programs at AspGD (http://www.aspergillusgenome.org/) and Broad Institute (http://www.broadinstitute.org/annotation/genome/aspergillus_group/MultiHome.html) databases. Reverse searches were performed to confirm the best putative homologue for each identified gene. Multiple alignments were done with ClustalX (Thompson *et al.*, 1997) and revised manually using GeneDoc software (http://iubio.bio.indiana.edu/soft/molbio/ibmpc/genedoc-readme.html). Phylogenetic and molecular evolutionary studies were performed using Mega software, version 4.0, neighbor-joining method, with a bootstrap of 50,000 replicates and the amino p-distance substitution model (Tamura *et al.*, 2007). Similarity, following Blosum62 matrix, and identity percentages were estimated using the complete amino acid sequence for all transporters.

Molecular techniques and generation of null and fluorescent-tagged strains

Strains carrying null alleles, GFP or cherry-mRFP C-terminally tagged fusions of nuclear transporters, and nuclear and nucleolar markers were generated as described (Yang *et al.*, 2004; Supplemental Figure S2), using *Aspergillus fumigatus pyrG*, *riboB*, or *pyroA* gene as a prototrophic selection marker. To construct an N-terminal GFP-tagged KapJ^{Kap123}, a null *kapJ*^{Kap123}::*pyrG*^{Af} strain was transformed with a 5′UTR::GFP::KapJ_{ORF}::3′UTR DNA cassette, and the replacement of the null locus was selected by growing the transformants in regeneration plates containing 2 mg/ml 5-fluoro-orotic acid (5-FOA; Apollo Scientific, Stockport, United Kingdom). After 24 h of incubation at 37°C, a layer of Aspergillus minimal medium containing the required nutrients and supplements plus 2 mg/ml FOA was poured onto the protoplast-regeneration plates. Colonies that grew through this layer of medium were purified to homokaryosis and analyzed by Southern blot to verify the correct integration of the cassette at the null *kapJ*^{Kap123} locus. Strains coexpressing tagged karyopherins and histone H1 (HhoA::mCh) or fibrillarin (An-Fib::mCh) were obtained by step-by-step transformation of MAD1425 with each fusion PCR cassette. Amplification of HhoA and An-Fib tagging cassettes follow standard procedures as described, but the selectable marker in this case was *A. fumigatus pyroA* gene. Strains MAD2653 (*kapL*^{Msn5}*::gfp*; *hhoA::mCh*) and MAD2654 (*kapI*^{Pse1}*::gfp*; *hhoA::mCh*) were obtained by transformation of MAD2446 with the karyopherin-tagging PCR cassette. Strains MAD3772 (*kapH*^{Kap120}*::gfp*; *nls::Dsred*) and MAD3771 (*kapI*^{Pse1}*::gfp*; *nls::Dsred*) were obtained by transformation of AY02 with the karyopherin-tagging PCR cassette. Strain MAD3817 is a diploid obtained from MAD3773 and MAD3604 haploid strains.

Oligonucleotides used in this study are summarized in Supplementary Table S2. Homologous recombination for each construct was confirmed by both diagnostic PCR and Southern blot analysis.

The expression of tagged proteins was analyzed by Western blotting using standard procedures. Briefly, *A. nidulans* strains were cultivated for 18 h in fermentation medium (Orejas *et al.*, 1995), filtered through Miracloth (Calbiochem, La Jolla, CA), squeezed to dry, frozen in dry ice, and lyophilized for 16 h. Protein extraction was carried out as previously described (Araújo-Bazán *et al.*, 2008), and 50 μg were loaded on an 8% polyacrylamide gel before electrotransfer to nitrocellulose filters. To detect GFP fusions, filters were incubated with anti-GFP mouse monoclonal antibody cocktail (1/5000; Roche, Indianapolis, IN). Actin, used as loading and extract quality control, was detected using mouse anti-actin antibody (1/50,000; ICN Biomedical, Irvine, CA). Peroxidase-conjugated anti-mouse (1/4000; Jackson ImmunoResearch Laboratories, West Grove, PA) was used as secondary antibody.

To characterize respective transporter coding sequence (CDS), cDNA was generated from total RNA extracted using TRIzol reagent (Invitrogen, Carlsbad, CA) and following the manufacturer's instructions. Total RNA was isolated from mycelia of a wild-type strain cultured under standard conditions. A single-strand cDNA library was made using the First-Strand cDNA Kit (Roche) and an oligo-dT primer. cDNA for each nuclear transporter was amplified using gene-specific oligonucleotides, and the CDS was confirmed by sequencing.

Fluorescence microscopy

Germlings were cultured in supplemented watch minimal medium (Peñalva, 2005), using uncoated glass-bottom dishes (MatTek

Corporation, Ashland, MA). Fluorescence images were acquired with an upright Eclipse 80i microscope (Nikon, Melville, NY) equipped with Brightline GFP-3035B and TXRED-4040B filter sets (Semrock, Rochester, NY), a 100-W mercury lamp epifluorescence module, a Uniblitz (Rochester, NY) external shutter, a 60× 1.40–numerical aperture (NA) plan apochromat objective, and an ORCA ERG camera (Hamamatsu, Bridgewater, NJ). In vivo imaging was performed at 37°C using a DMI6000B inverted microscope (Leica, Deerfield, IL) equipped with a heating insert P (PeCon, Erbach, Germany), a Hamamatsu ORCA ER-II camera, an EL6000 external light source for epifluorescence excitation, an HCX 63× 1.4 NA objective, and Semrock Brightline GFP-3035B and TXRED-4040B (mRFP) filter sets. Kymographs, contrast adjustment, color combining, and z-stack maximal intensity projections were made using Metamorph (Molecular Devices, Sunnyvale, CA). Deconvolution was made using AutoDeblur software (Media Cybernetics, Bethesda, MD) and a blind deconvolution setup. Time-lapse sequences were converted to QuickTime format using ImageJ 1.37 software (National Institutes of Health, Bethesda, MD).

Nuclei were visualized using mCherry-tagged histone H1 (HhoA; Etxebeste *et al.*, 2009, and references therein) or with DAPI staining. An-Fib (AN0745.3), an rRNA 2′-*O*-methyltransferase similar to *S. cerevisiae* Nop1 and vertebrate fibrillarin, was used as a marker for nucleolar positioning and disassembly process (Ukil *et al.*, 2009). Nud1 tagged with mCh (Xiong and Oakley, 2009) was used for labeling the position of spindle pole bodies. Active nuclear transport during mitosis was followed using the StuA NLS fused to the DsRed fluorescent protein as a reporter whose expression is driven by the constitutive promoter *gpdA* (Suelmann *et al.*, 1997; Ukil *et al.*, 2009).

ACKNOWLEDGMENTS

This work was supported by the Spanish Ministerio de Educación y Ciencia through grants BFU2006-04185 and BFU2009-08701 to E.A.E. A.M.-I. held a predoctoral FPI fellowship from the Ministerio de Educación y Ciencia associated with Grant BIO2006-00556 to Miguel A. Peñalva. O.E. held a research contract associated with Grant BFU2006-04185 at the Centro de Investigaciones Biológicas and is now a contract researcher of the University of the Basque Country with funds from the Diputación Foral de Gipuzkoa (SA-2010/00105), the Basque Government (IT393-10), and the Ministerio de Educación y Ciencia (BFU2010-17528). L.A.-B. was a predoctoral fellow of the Formación de Profesorado Universitario program of the Spanish Ministerio de Ciencia y Tecnología. E.H.-G. held a predoctoral fellowship from the Basque Government. This work was also supported by National Institutes of Health Grant GM042564 to S.A.O.

REFERENCES

Araújo-Bazán L, Dhingra S, Chu J, Fernandez-Martinez J, Calvo AM, Espeso EA (2009). Importin alpha is an essential nuclear import carrier adaptor required for proper sexual and asexual development and secondary metabolism in *Aspergillus nidulans*. Fungal Genet Biol 46, 506–515.

Araújo-Bazán L, Fernandez-Martinez J, Rios VM, Etxebeste O, Albar JP, Peñalva MA, Espeso EA (2008). NapA and NapB are the *Aspergillus nidulans* Nap/SET family members and NapB is a nuclear protein specifically interacting with importin alpha. Fungal Genet Biol 45, 278–291.

Bayram O *et al.* (2008). VelB/VeA/LaeA complex coordinates light signal with fungal development and secondary metabolism. Science 320, 1504–1506.

Bernreiter A *et al.* (2007). Nuclear export of the transcription factor NirA is a regulatory checkpoint for nitrate induction in *Aspergillus nidulans*. Mol Cell Biol 27, 791–802.

Bischoff FR, Krebber H, Smirnova E, Dong W, Ponstingl H (1995). Co-activation of RanGTPase and inhibition of GTP dissociation by Ran-GTP binding protein RanBP1. EMBO J 14, 705–715.

Chook YM, Blobel G (2001). Karyopherins and nuclear import. Curr Opin Struct Biol 11, 703–715.W

Clutterbuck AJ (1993). *Aspergillus nidulans, nuclear genes*, In: Genetic Maps: Locus Maps of Complex Genomes, 6th ed., ed. SJ O'Brien, New York: Cold Spring Harbor Laboratory Press, 371–384.

Conti E, Izaurralde E (2001). Nucleocytoplasmic transport enters the atomic age. Curr Opin Cell Biol 13, 310–319.

Cronshaw JM, Krutchinsky AN, Zhang W, Chait BT, Matunis MJ (2002). Proteomic analysis of the mammalian nuclear pore complex. J Cell Biol 158, 915–927.

De Souza CP, Osmani AH, Hashmi SB, Osmani SA (2004). Partial nuclear pore complex disassembly during closed mitosis in *Aspergillus nidulans*. Curr Biol 14, 1973–1984.

De Souza CP, Osmani SA (2007). Mitosis, not just open or closed. Eukaryot Cell 6, 1521–1527.

Espeso EA, Osmani SA (2008). Nuclear pore complex and transport in *Aspergillus nidulans*. In: The Aspergilli: Genomics, Medical Aspects, Biotechnology and Research Methods, ed. GH Goldman and SA Osmani, Boca Raton, FL: CRC Press, 261–274.

Etxebeste O, Markina-Inarrairaegui A, Garzia A, Herrero-Garcia E, Ugalde U, Espeso EA (2009). KapI, a non-essential member of the Pse1p/Imp5 karyopherin family, controls colonial and asexual development in *Aspergillus nidulans*. Microbiology 155, 3934–3945.

Etxebeste O, Ni M, Garzia A, Kwon NJ, Fischer R, Yu J-H, Espeso EA, Ugalde U (2008). Basic-Zipper-type transcription factor FlbB controls asexual development in *Aspergillus nidulans*. Eukaryotic Cell 7, 38–48.

Fernandez-Martinez J, Brown CV, Diez E, Tilburn J, Arst HN Jr, Penalva MA, Espeso EA (2003). Overlap of nuclear localisation signal and specific DNA-binding residues within the zinc finger domain of PacC. J Mol Biol 334, 667–684.

Fiserova J, Goldberg MW (2010). Nucleocytoplasmic transport in yeast: a few roles for many actors. Biochem Soc Trans 38, 273–277.

Fornerod M, Ohno M, Yoshida M, Mattaj IW (1997). CRM1 is an export receptor for leucine-rich nuclear export signals. Cell 90, 1051–1060.

Fribourg S, Braun IC, Izaurralde E, Conti E (2001). Structural basis for the recognition of a nucleoporin FG repeat by the NTF2-like domain of the TAP/p15 mRNA nuclear export factor. Mol Cell 8, 645–656.

Fribourg S, Conti E (2003). Structural similarity in the absence of sequence homology of the messenger RNA export factors Mtr2 and p15. EMBO Rep 4, 699–703.

Gorlich D, Kutay U (1999). Transport between the cell nucleus and the cytoplasm. Annu Rev Cell Dev Biol 15, 607–660.

Grant RP, Neuhaus D, Stewart M (2003). Structural basis for the interaction between the Tap/NXF1 UBA domain and FG nucleoporins at 1A resolution. J Mol Biol 326, 849–858.

Kadowaki T, Chen S, Hitomi M, Jacobs E, Kumagai C, Liang S, Schneiter R, Singleton D, Wisniewska J, Tartakoff AM (1994). Isolation and characterization of *Saccharomyces cerevisiae* mRNA transport-defective (mtr) mutants. J Cell Biol 126, 649–659.

Kalab P, Heald R (2008). The RanGTP gradient—a GPS for the mitotic spindle. J Cell Sci 121, 1577–1586.

Kalderon D, Roberts BL, Richardson WD, Smith AE (1984). A short amino acid sequence able to specify nuclear location. Cell 39, 499–509.

Kosugi S, Hasebe M, Matsumura N, Takashima H, Miyamoto-Sato E, Tomita M, Yanagawa H (2009). Six classes of nuclear localization signals specific to different binding grooves of importin α. J Biol Chem 284, 478–485.

la Cour T, Kiemer L, Molgaard A, Gupta R, Skriver K, Brunak S (2004). Analysis and prediction of leucine-rich nuclear export signals. Protein Eng Des Sel 17, 527–536.

Macara IG (2001). Transport into and out of the nucleus. Microbiol Mol Biol Rev 65, 570–94, table.

Madrid AS, Weis K (2006). Nuclear transport is becoming crystal clear. Chromosoma 115, 98–109.

Makkerh JP, Dingwall C, Laskey RA (1996). Comparative mutagenesis of nuclear localization signals reveals the importance of neutral and acidic amino acids. Curr Biol 6, 1025–1027.

Mans BJ, Anantharaman V, Aravind L, Koonin EV (2004). Comparative genomics, evolution and origins of the nuclear envelope and nuclear pore complex. Cell Cycle 3, 1612–1637.

Mattaj IW, Englmeier L (1998). Nucleocytoplasmic transport: the soluble phase. Annu Rev Biochem 67, 265–306.

Mingot JM, Kostka S, Kraft R, Hartmann E, Gorlich D (2001). Importin 13: a novel mediator of nuclear import and export. EMBO J 20, 3685–3694.

Mosammaparast N, Pemberton LF (2004). Karyopherins: from nuclear-transport mediators to nuclear-function regulators. Trends Cell Biol 14, 547–556.
Murthi A, Shaheen HH, Huang HY, Preston MA, Lai TP, Phizicky EM, Hopper AK (2010). Regulation of tRNA bidirectional nuclear-cytoplasmic trafficking in *Saccharomyces cerevisiae*. Mol Biol Cell 21, 639–649.
Nayak T, Szewczyk E, Oakley CE, Osmani A, Ukil L, Murray SL, Hynes MJ, Osmani SA, Oakley BR (2006). A versatile and efficient gene-targeting system for *Aspergillus nidulans*. Genetics 172, 1557–1566.
Neville M, Rosbash M (1999). The NES-Crm1p export pathway is not a major mRNA export route in *Saccharomyces cerevisiae*. EMBO J 18, 3746–3756.
Nguyen Ba AN, Pogoutse A, Provart N, Moses AM (2009). NLStradamus: a simple hidden Markov model for nuclear localization signal prediction. BMC Bioinformatics 10, 202.
Ohtsubo M, Okazaki H, Nishimoto T (1989). The RCC1 protein, a regulator for the onset of chromosome condensation locates in the nucleus and binds to DNA. J Cell Biol 109, 1389–1397.
Orejas M, Espeso EA, Tilburn J, Sarkar S, Arst HN Jr, Peñalva MA (1995). Activation of the *Aspergillus* PacC transcription factor in response to alkaline ambient pH requires proteolysis of the carboxy-terminal moiety. Genes Dev 9, 1622–1632.
Osmani AH, Davies J, Liu HL, Nile A, Osmani SA (2006a). Systematic deletion and mitotic localization of the Nuclear Pore Complex proteins of *Aspergillus nidulans*. Mol Biol Cell 17, 4946–4961.
Osmani AH, Oakley BR, Osmani SA (2006b). Identification and analysis of essential *Aspergillus nidulans* genes using the heterokaryon rescue technique. Nat Protoc 1, 2517–2526.
Ossareh-Nazari B, Bachelerie F, Dargemont C (1997). Evidence for a role of CRM1 in signal-mediated nuclear protein export. Science 278, 141–144.
Pemberton LF, Paschal BM (2005). Mechanisms of receptor-mediated nuclear import and nuclear export. Traffic 6, 187–198.
Peñalva MA. (2005). Tracing the endocytic pathway of *Aspergillus nidulans* with FM4-64. Fungal Genet Biol 42, 963–975.
Peñalva MA, Tilburn J, Bignell E, Arst HN Jr (2008). Ambient pH gene regulation in fungi: making connections. Trends Microbiol 16, 291–300.
Petosa C, Schoehn G, Askjaer P, Bauer U, Moulin M, Steuerwald U, Soler-Lopez M, Baudin F, Mattaj IW, Muller CW (2004). Architecture of CRM1/Exportin1 suggests how cooperativity is achieved during formation of a nuclear export complex. Mol Cell 16, 761–775.
Polizotto RS, Cyert MS (2001). Calcineurin-dependent nuclear import of the transcription factor Crz1p requires Nmd5p. J Cell Biol 154, 951–960.
Ribbeck K, Gorlich D (2002). The permeability barrier of nuclear pore complexes appears to operate via hydrophobic exclusion. EMBO J 21, 2664–2671.
Robbins J, Dilworth SM, Laskey RA, Dingwall C (1991). Two interdependent basic domains in nucleoplasmin nuclear targeting sequence: identification of a class of bipartite nuclear targeting sequence. Cell 64, 615–623.
Rout MP, Aitchison JD, Suprapto A, Hjertaas K, Zhao Y, Chait BT (2000). The yeast nuclear pore complex: composition, architecture, and transport mechanism. J Cell Biol 148, 635–651.
Rout MP, Blobel G, Aitchison JD (1997). A distinct nuclear import pathway used by ribosomal proteins. Cell 89, 715–725.
Ryan KJ, Wente SR (2000). The nuclear pore complex: a protein machine bridging the nucleus and cytoplasm. Curr Opin Cell Biol 12, 361–371.
Seedorf M, Silver PA (1997). Importin/karyopherin protein family members required for mRNA export from the nucleus. Proc Natl Acad Sci USA 94, 8590–8595.
Segref A, Sharma K, Doye V, Hellwig A, Huber J, Luhrmann R, Hurt E (1997). Mex67p, a novel factor for nuclear mRNA export, binds to both poly(A)+ RNA and nuclear pores. EMBO J 16, 3256–3271.
Senger B, Simos G, Bischoff FR, Podtelejnikov A, Mann M, Hurt E (1998). Mtr10p functions as a nuclear import receptor for the mRNA-binding protein Npl3p. EMBO J 17, 2196–2207.
Spielvogel A, Findon H, Arst HN Jr, Araújo-Bazán L, Hernandez-Ortiz P, Stahl U, Meyer V, Espeso EA (2008). Two zinc finger transcription factors, CrzA and SltA, are involved in cation homoeostasis and detoxification in *Aspergillus nidulans*. Biochem J 414, 419–429.
Stade K, Ford CS, Guthrie C, Weis K (1997). Exportin 1 (Crm1p) is an essential nuclear export factor. Cell 90, 1041–1050.
Stinnett SM, Espeso EA, Cobeno L, Araujo-Bazan L, Calvo AM (2007). *Aspergillus nidulans* VeA subcellular localization is dependent on the importin alpha carrier and on light. Mol Microbiol 63, 242–255.
Strom AC, Weis K (2001). Importin-beta-like nuclear transport receptors. Genome Biol 2, reviews 3008.
Suelmann R, Sievers N, Fischer R (1997). Nuclear traffic in fungal hyphae: in vivo study of nuclear migration and positioning in *Aspergillus nidulans*. Mol Microbiol 25, 757–769.
Suntharalingam M, Wente SR (2003). Peering through the pore: nuclear pore complex structure, assembly, and function. Dev Cell 4, 775–789.
Sydorskyy Y, Dilworth DJ, Yi EC, Goodlett DR, Wozniak RW, Aitchison JD (2003). Intersection of the Kap123p-mediated nuclear import and ribosome export pathways. Mol Cell Biol 23, 2042–2054.
Taberner FJ, Igual JC (2010). Yeast karyopherin Kap95 is required for cell cycle progression at Start. BMC Cell Biol 11, 47.
Tamura K, Dudley J, Nei M, Kumar S (2007). MEGA4: Molecular Evolutionary Genetics Analysis (MEGA) software version 4.0. Mol Biol Evol 24, 1596–1599.
Terry LJ, Wente SR (2009). Flexible gates: dynamic topologies and functions for FG nucleoporins in nucleocytoplasmic transport. Eukaryot Cell 8, 1814–1827.
Thompson JD, Gibson TJ, Plewniak F, Jeanmougin F, Higgins DG (1997). The CLUSTAL_X windows interface: flexible strategies for multiple sequence alignment aided by quality analysis tools. Nucleic Acids Res 25, 4876–4882.
Titov AA, Blobel G (1999). The karyopherin Kap122p/Pdr6p imports both subunits of the transcription factor IIA into the nucleus. J Cell Biol 147, 235–246.
Todd RB, Fraser JA, Wong KH, Davis MA, Hynes MJ (2005). Nuclear accumulation of the GATA factor AreA in response to complete nitrogen starvation by regulation of nuclear export. Eukaryot Cell 4, 1646–1653.
Ukil L, De Souza CP, Liu HL, Osmani SA (2009). Nucleolar separation from chromosomes during *Aspergillus nidulans* mitosis can occur without spindle forces. Mol Biol Cell 20, 2132–2145.
Weis K (2002). Nucleocytoplasmic transport: cargo trafficking across the border. Curr Opin Cell Biol 14, 328–335.
Wong J *et al*. (2007). A protein interaction map of the mitotic spindle. Mol Biol Cell 18, 3800–3809.
Xiong Y, Oakley BR (2009). In vivo analysis of the functions of gamma-tubulin-complex proteins. J Cell Sci 122, 4218–4227.
Yang L, Ukil L, Osmani A, Nahm F, Davies J, De Souza CP, Dou X, Perez-Balaguer A, Osmani SA (2004). Rapid production of gene replacement constructs and generation of a green fluorescent protein-tagged centromeric marker in *Aspergillus nidulans*. Eukaryotic Cell 3, 1359–1362.
Yao W, Lutzmann M, Hurt E (2008). A versatile interaction platform on the Mex67-Mtr2 receptor creates an overlap between mRNA and ribosome export. EMBO J 27, 6–16.
Yoshida K, Blobel G (2001). The karyopherin Kap142p/Msn5p mediates nuclear import and nuclear export of different cargo proteins. J Cell Biol 152, 729–740.
Zenklusen D, Stutz F (2001). Nuclear export of mRNA. FEBS Lett. 498, 150–156.